Cement and Concrete Research 38 (2008) 1190–1196

Contents lists available at ScienceDirect

Cement and Concrete Research

journal homepage: http://ees.elsevier.com/CEMCON/default.asp

Effect of aggregates and microcracks on the drying rate of cementitious composites

Jan Bisschop *, Jan G.M. van Mier

ETH Zürich, Institute for Building Materials, Dept. of Civil, Environmental and Geomatic Engineering, 8093 Zürich, Switzerland

ARTICLE INFO

Article history:
Received 14 September 2007
Accepted 21 March 2008

Keywords:
Drying shrinkage
Diffusion
Aggregates
Microcracking
Effective composite properties

ABSTRACT

We investigated the effect of aggregate concentration on the drying rate of cementitious composites with glass beads, sand grains, or expanded polystyrene (EPS) beads as aggregates. The drying rate of composites with non-diffusive aggregates (glass beads and sand grains) decreased with aggregate concentration. Composites with 60% glass beads dried a factor 1.3 slower than plain cement paste with the same w/c-ratio. Composites with EPS-beads showed the opposite trend: an increased drying rate for composites with higher aggregate concentrations. However, the effective diffusion coefficients of the EPS-composites decreased with increasing aggregate concentration. A higher aggregate concentration means that less water needs to diffuse out of the material to reach a specific degree of drying, and this effect mainly determined the drying rate of the composites with EPS-beads. The development of drying shrinkage microcracks had a small effect on the drying rate of the studied composites.

1. Introduction

Moisture transport properties of cementitious composite materials (concrete and mortar) have been widely studied, since they partially determine the durability of these building materials. Permeation of rain, soil, or sea water into concrete may accelerate the ingress of dissolved ions such as Cl^- and SO_4^{2-}, and lead to corrosion of the steel reinforcement bars or to sulfate attack, respectively. The reverse process, drying of concrete, also affects the durability of the material, since it generally leads to drying shrinkage (micro)cracking. Drying of cementitious materials is a transient water evaporation and water vapour diffusion process driven by a difference in relative humidity between the material and its environment.

The bulk diffusion coefficient (D_{bulk}) of a cementitious composite is a function of the diffusion coefficients of the matrix (D_m) and aggregates (D_a), and the aggregate volume fraction (g_a) as shown for three different models in Fig. 1. The first model (Eq. (1)) is a composite sphere model that has originally been derived for electrical conductivity and magnetic permeability of multiphase materials [1,2]. Due to mathematical analogy the model also holds for the dielectric constant, heat conductivity, and diffusivity [1]. The second model (Eq. (2)) is a simple linear rule of mixtures, that does not take into account the longer (tortuous) diffusion path in composites with non-diffusive aggregates. When $0.5 < D_a/D_m > 1.5$ Eqs. (1) and (2) give similar results. The last model (Eq. (3)) is the Bruggeman–Hanai (B–H) law for the case of spherical, nonconductive particles in a conductive matrix [3], and can possibly be used for predicting the effective moisture diffusivity of concretes with dense, non-diffusive aggregates.

There are other factors that could affect water vapour transport in cementitious composites upon drying. Drying of cementitious materials is accompanied by shrinkage of the material, and this leads to stresses and (micro)cracks when the shrinkage is restraint. Bažant et al. [4] showed experimentally that drying rate in concrete specimen with (macro)cracks was a factor 2.25 higher than in the uncracked control specimens. A number of theoretical studies have also shown that drying shrinkage cracks or loading cracks may accelerate the drying rate of cementitious materials [5–7]. Other theoretical studies predict no or a minor effect of (micro)cracks on diffusive transport [8,9]. Also the presence of an interfacial transition zone (ITZ) around the aggregates could have an effect on the transport properties of concrete. The ITZ may be a few tens of μm's thick and have a porosity of up to twice as large as the bulk matrix [10], and for this reason is likely to have a higher local diffusion coefficient. Above a certain aggregate volume fraction the ITZ-zones between neighboring aggregates may overlap and form a percolating network in the material that could increase the rate of transport through cementitious composites [3,11,12].

Previously we have investigated how aggregates affect drying shrinkage microcracking in cementitious composites [13,14]. In this paper we investigate how aggregates and microcracks affect the drying rate of these composites with equal water–cement ratio. We worked with model aggregates (sand grains, glass beads, or polystyrene beads) that varied in mechanical and transport properties. These 'extreme' model mixtures, that are unlikely building materials themselves, clearly

* Corresponding author. Tel.: +41 446337135.
E-mail address: jbisschop@ethz.ch (J. Bisschop).

0008-8846/$ – see front matter © 2008 Elsevier Ltd. All rights reserved.
doi:10.1016/j.cemconres.2008.03.015

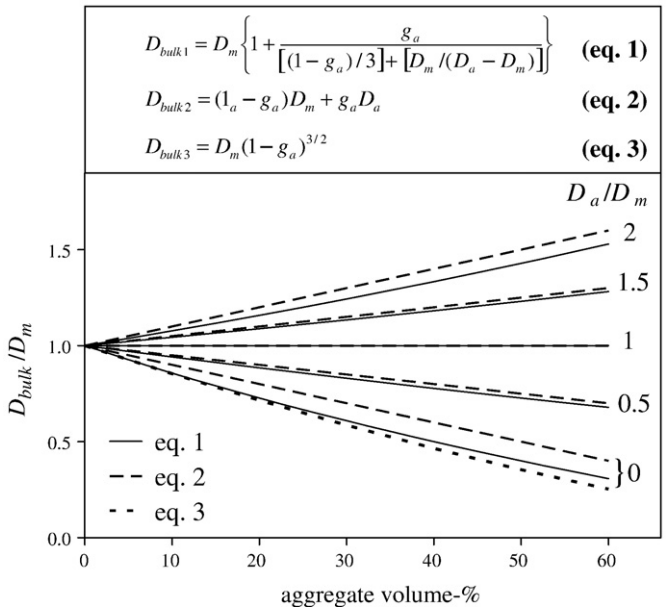

Fig. 1. Model effects of aggregate concentration and aggregate diffusivity on effective bulk diffusivity of composite materials with spherical aggregates (see text for discussion).

show what determines the effective moisture transport properties of cementitious composites.

2. Methods

2.1. Materials

The matrix of all cementitious composites in this investigation consisted of CEM I 52.5R cement with a water–cement ratio of 0.45. The chemistry of the cement is given in [13]. A total of 33 composite types have been studied to investigate the effect of aggregate content on: (i) moisture absorption during wet-curing; (ii) drying shrinkage microcracking; and (iii) drying rate (see Table 1). In the composites label the first capital stands for the aggregate type: G for glass beads, N for natural sand (quartz, feldspar) grains, and PS for expanded polystyrene (EPS) beads. The number in the label (0.5, 1, 2, 4, or 6) stands for the round-off diameter (in mm) of the mono-sized aggregates. Actual average glass bead sizes were 0.54; 1.1; 2.3; 3.8; and 5.9 mm. The number behind the hyphen (e.g., 10, 21, or 35) gives the quantity of aggregates, expressed as the aggregate volume percentage. In composite G6r-35, and G4r-35 the glass spheres were roughened by sandblasting (*r* is added in label) to increase the bond strength between aggregates and matrix. A number of mixtures with Fuller graded (fg) or gap graded (gg) aggregates (glass beads or sand grains) with maximum aggregate size of 6 mm were studied as well. For most mixtures, 3 samples were cast in order to measure drying shrinkage microcracking at 3 different stages of drying. In some cases up to 7 or 21 specimens were cast to determine the reproducibility of the measurements.

2.2. Casting and conditioning

After stirring the mixtures for 3 minutes in a Hobart mixer they were cast in prismatic moulds of 40×40×160 mm. The moulds were sealed with three layers of plastic foil sheets and stored for 24 h at room temperature. Then, the prisms were demoulded, weighted, and placed vertically in a container with calciumhydroxide saturated tap water for 6 days at room temperature. At an age of 7 days, the specimens were removed from the water and their weight was recorded after removing water drops from the specimen surfaces. Immediately after weighing, all sides except the top surface of the specimens were sealed with three layers of adhesive tape. The top surface (drying surface) was the former bottom surface of the specimen in the mould. Thus, only one side of the specimens were exposed to drying to create one-dimensional drying. After sealing, the initial weight of specimens (including the tape) was recorded. Then, the specimens were placed in an environmental cabin to start the drying experiments. The environmental cabin (a Lab-line® Environ-Cab™) was ventilated with air with a temperature of 31.0 °C±0.5 °C and relative humidity of 31%±3%. The weights of the specimens was frequently measured for over a drying period of 4–6 months. The drying curves of most of the studied composites can be found in [13,14].

2.3. Drying rate measurements

For a given driving force, the transport rate of moisture through cementitious composites is given by the effective diffusion coefficients (in m^2/s) or effective permeabilities (in kg/m·s·Pa). In this paper we will show that the drying rate of cementitious materials is not only a function of the effective transport rate coefficient, but also depends on the total amount of water that needs to be transported to reach a specific degree of drying. We define a *degree of drying* as the moisture loss relative to the initial moisture content of the material. For example, a degree of drying of 10% means that 10% of the initial moisture content was lost. The measured time required to reach three different drying stages (10, 20, and 30% degree of drying) is used in this paper as a measure for the average drying rate of the cementitious composites.

The water-cement ratio was the same for all studied cementitious composites, and therefore the initial moisture content was linearly related to the matrix volume percentage of these composites. The initial or added water content of the mixture is not equal to the free water content at the start of the drying experiment, because the cement reacted with water and the specimens absorbed water during 6 days of wet-curing. The water absorption was linearly related to the matrix volume (see Section 3.1), and it is not expected that the rate of hydration varied much among the studied composites. For these reasons, the free water content of all composites at the start of the drying experiments was approximately proportional to the matrix volume percentage. The degree of drying is thus simply a measure of the moisture loss normalized against the matrix volume percentage.

2.4. Microcrack detection and quantification

Drying shrinkage microcracking was measured at degrees of drying of 10, 20, and 30%. A detailed description of the optical microscopy method to detect and quantify drying shrinkage microcracks on a specimen cross-

Table 1
Studied cementitious composites, *n* is the number of specimens, and the number in between brackets indicates if the used cement was from bag 1 or 2

Mixture	*n*	Mixture	*n*	Mixture	*n*	Mixture	*n*	Mixture	*n*
P	21 *(1,2)*	G2-10	7 *(1)*	G6-10	7 *(1)*	Ggg1-59	3 *(2)*	N6-35	3 *(2)*
G0.5-10	3 *(1)*	G2-21	3 *(1)*	G6-21	3 *(1)*	Ggg2-59	3 *(2)*	Nfg-14	3 *(2)*
G0.5-21	3 *(1)*	G2-35	3 *(1)*	G6-35	6 *(1,2)*			Nfg-35	3 *(2)*
G0.5-35	3 *(1)*	G4-10	3 *(1)*	G6r-35	3 *(2)*	PS4-10	3 *(2)*	Nfg-59	3 *(2)*
G1-10	3 *(1)*	G4-21	3 *(1)*	Gfg-14	3 *(2)*	PS4-21	3 *(2)*	Ngg1-59	3 *(2)*
G1-21	3 *(1)*	G4-35	6 *(1,2)*	Gfg-35	3 *(2)*	PS4-35	3 *(2)*	Ngg2-59	3 *(2)*
G1-35	3 *(1)*	G4r-35	3 *(2)*	Gfg-59	6 *(2)*	PS6-35	3 *(2)*		

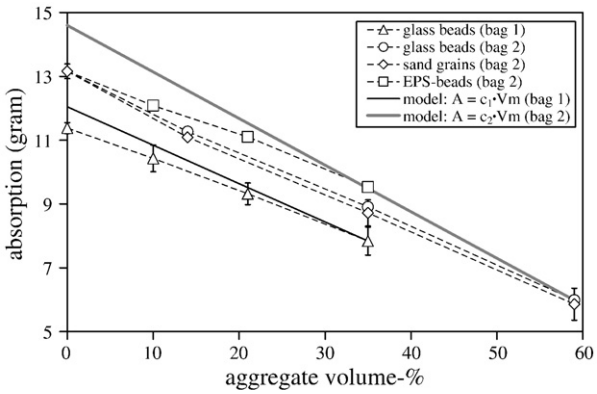

Fig. 2. Moisture absorption of composites with glass beads, sand grains or expanded polystyrene (EPS) beads after 6 days wet-curing. Error bars for composites with EPS-beads are smaller than the data-icons.

section can be found in [13,15]. To avoid recording microcracks introduced by sample preparation, the dried specimens were impregnated with a fluorescent epoxy before sectioning. The microcracks were then very clearly visible under the microscope in the fluorescent light mode. The microcracks were manually mapped on a printout (reference map) of the digital microscope recordings while sitting behind the microscope examining the specimens. The traced microcracks were redrawn on the computer screen with a mouse to obtain the digital crack maps. Drying shrinkage microcracks were quantified by measuring the total cumulative length of cracks in the digital crack-maps (excluding bond cracks), and the maximum crack depth in the specimen. Measurements of 4 sections of 40 x 40 mm^2 were averaged.

3. Results

3.1. Moisture absorption during wet-curing

The moisture absorption during 6 days wet-curing as function of the aggregate concentration is given in Fig. 2. After 6 days wet-curing, the specimens reached about 75% of the equilibrium absorbed moisture content measured after 150 days [13]. All composites were cast in two series from two different bags of the same cement batch. The moisture absorption of specimens prepared with cement from bag 1 was systematically lower than those prepared from bag 2 (Fig. 2). The absorption of composites with glass beads, sand grains or EPS beads almost linearly increased with matrix volume percentage. Also shown in Fig. 2 are theoretical curves (solid lines) for absorption (A) only being a linear function of matrix volume percentage (V_m), i.e., $A = c \cdot V_m$. The slopes of the experimental absorption curves are lower than the theoretical ones. This difference may have been caused by the moisture absorption *rate*, since the specimens did not reach absorbed moisture equilibrium. The relative moisture absorption rate may have increased with aggregate concentration, and thereby have caused the lower relative moisture absorption for specimens with fewer aggregates. The higher moisture absorption of the composites with EPS beads is likely to be a result of the higher moisture permeability and capacity of EPS compared to that of glass or sand.

3.2. Effect of microcracks on drying rate

Drying leads to shrinkage of the cement paste matrix. Drying shrinkage microcracks as shown in Fig. 3 were a result of two types of internal restraints against the matrix shrinkage: (i) Self-restraint occurs due to the development of a steep moisture gradient (and corresponding shrinkage gradient) upon drying and leads to micro-cracks perpendicular to the drying surface (Fig. 3a); (ii) Aggregate-restraint is a result of the stiffness-contrast between the aggregates and the matrix. The higher the aggregate stiffness or larger the aggregate particles, the more microcracks develop upon drying (Fig. 3b,c). The effect of aggregate type and concentration on drying shrinkage microcracking has been described in detail before [13,14]. In this paper we investigate if the quantity of microcracks had an influence on the drying rate of the composites. The microcrack width varied from maximum values of 30 μm in plain cement paste (near the drying surface) to around 1–5 μm in composites with high aggregate concentrations.

In composites with glass beads, larger total crack length and maximum crack depth resulted in a slightly higher drying rate, i.e., lower drying time to reach 10 or 20% degree of drying, as shown by best linear fits through the data points (Fig. 4). Total crack length and maximum crack depth were roughly linearly related and therefore their effects on drying rate were similar. In many composites the maximum crack depth stayed below 10 mm at all three stages of drying, and in these composites the increase in crack length with degree of drying was relatively small. In these composites it is therefore expected that the effect of cracking on drying rate was strongest at the start of drying (10% degree of drying) and weaker at later stages of drying (20 or 30% degree of drying). This may be the reason that the slope of the best-fits did not increase (i.e., became more negative) with degree of drying. In fact, the slope of the best-fit line decreased slightly from 10 to 20% degree of drying and was almost horizontal at 30% degree of drying. The large scatter of the data at 30% degree of drying is a result of the effect of aggregate

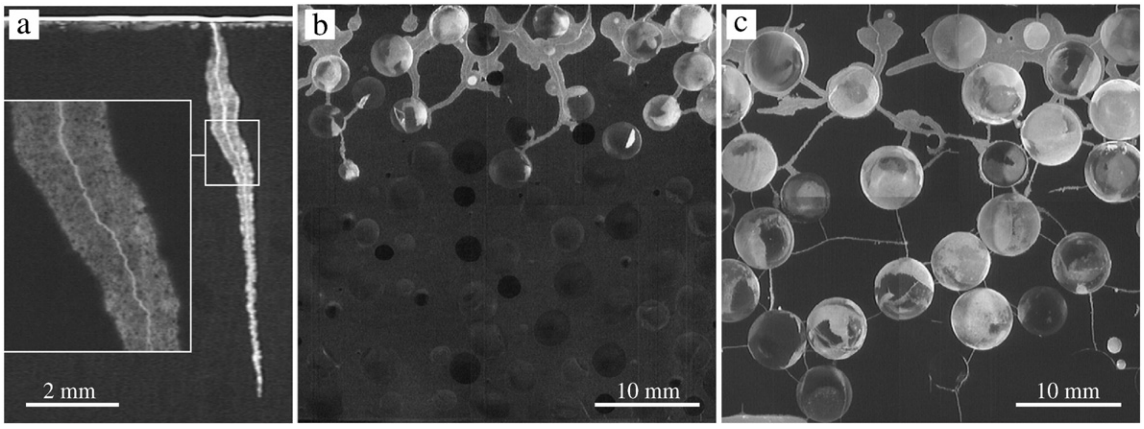

Fig. 3. Drying shrinkage microcracking on cross-sections through cementitious composites (impregnated with a fluorescent epoxy before sectioning). All 3 samples dried at 31 °C and 31% RH until they lost 20% of their initial moisture contents. (a.) Plain hardened cement paste; (b.) composite with 4 mm glass beads; and (c.) composite with 6 mm glass beads.

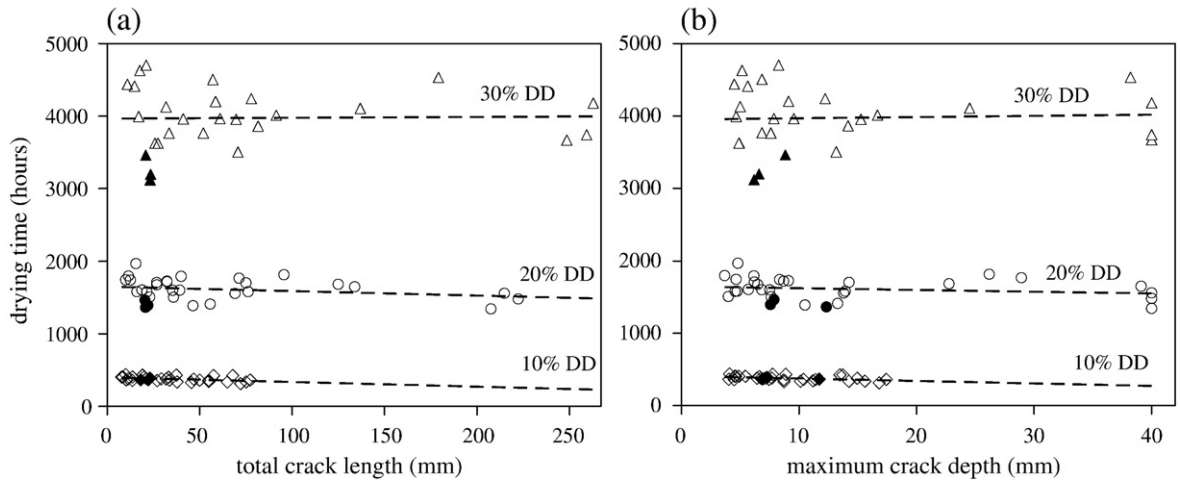

Fig. 4. Effect of drying shrinkage microcracking on the drying time (drying rate) of cementitious composites with glass beads. (a.) Effect of the total crack length; and (b.) effect of maximum crack depth. The height of the specimens was 40 mm. The filled icons represent the plain cement paste specimens. The dashed lines are linear best-fits. DD is degree of drying.

concentration on drying rate, which increased with degree of drying (see Section 3.4).

3.3. Effect aggregate size on drying rate

The effect of aggregate (glass bead) size on drying rate of composites with glass beads was very small or absent as shown by best linear fits through the data points (Fig. 5). The data points in Fig. 5 represent the average drying time of 3 specimens with a aggregate concentrations of 10, 21, and 35%. Again, the scatter of the data increased with degree of drying due to an increased effect of aggregate concentration on drying rate (Section 3.4). The slightly lower drying times for composites with 4 and 6 mm beads (at 10 and 20% drying) could be a result of the much higher crack densities in these composites. There is no theoretical effect of aggregate size on the bulk diffusion coefficient of composites (D_{bulk}) with spherical aggregates (Fig. 1). It is therefore likely that *aggregate size distribution* has no large effect on the drying rate of cementitious composites as well.

3.4. Effect aggregate diffusivity and concentration on drying rate

Aggregate concentration had a significant effect on the drying time required to reach 10, 20, or 30% degree of drying in all studied types of cementitious composites (Figs. 6–8). Higher concentrations of glass beads or sand grains generally meant longer drying times, but higher concentrations of EPS-beads lead to lower drying times. The drying time required to reach a specific degree of drying in cementitious composites is a trade off between: (i) the bulk diffusion coefficient of the composite (D_{bulk}), and (ii.) the total amount of moisture that needs to be transported out of the specimen. On the one hand, higher concentrations of aggregates will result in a lower bulk diffusion coefficient (D_{bulk}) when $D_a < D_m$ (see Fig. 1). On the other hand, a higher concentration of aggregates will reduce the matrix volume percentage and thus the absolute amount of water that needs to be transported out of the specimen to reach a specific degree of drying. In the Appendix we give a simple linear diffusion model predicting that the drying time required to reach a specific degree of drying, is proportional to the total moisture loss divided by the bulk diffusion coefficient ($t \sim m_t / D_{\text{bulk}}$). The drying times that are predicted by this model are given by thick solid lines in Figs. 6–8.

For the glass bead composites the simple model reproduces the global increasing trend in drying time with aggregate concentration when we choose zero diffusivity for the glass beads ($D_a/D_m = 0$) as shown in Fig. 6. The drying times at aggregate-volume percentages of 10 and 14% were, however, significantly higher than the predicted values. The height of this 'bump' in the experimental curve increased with the slope of the curve from 10 to 30% degree of drying. The reason for these relatively low drying rates at low aggregate concentrations is not understood. The drying behaviour of sand grain composites

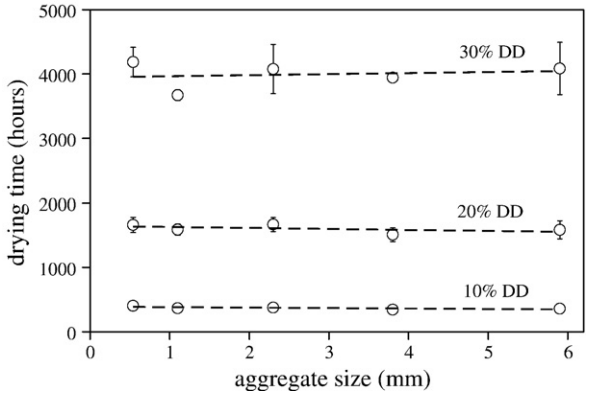

Fig. 5. Effect of aggregate (glass bead) size on the drying time (drying rate) of cementitious composites. Error bars at a 10% degree of drying (DD) are smaller than the data-icons.

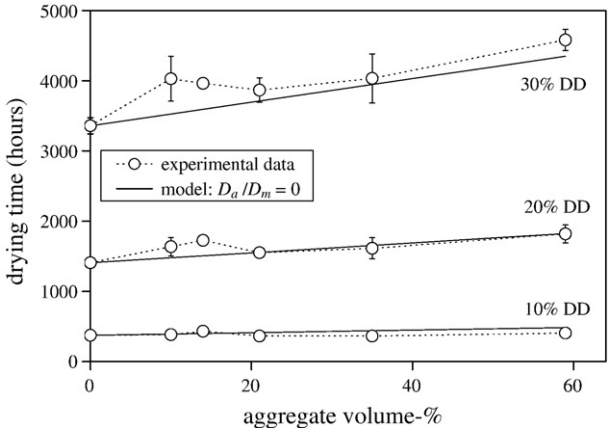

Fig. 6. Effect of aggregate concentration on the drying time (drying rate) of glass bead composites (mono-sized or graded, see Table 1). Number of specimens were as follows for aggregate concentrations of 0% ($n=4$); 10% ($n=9$), 14% ($n=1$); 21% ($n=5$); 35% ($n=10$); and 59% ($n=3$) for all stages of drying. Error bars of data points at 10% degree of drying (DD) smaller than the data-icons.

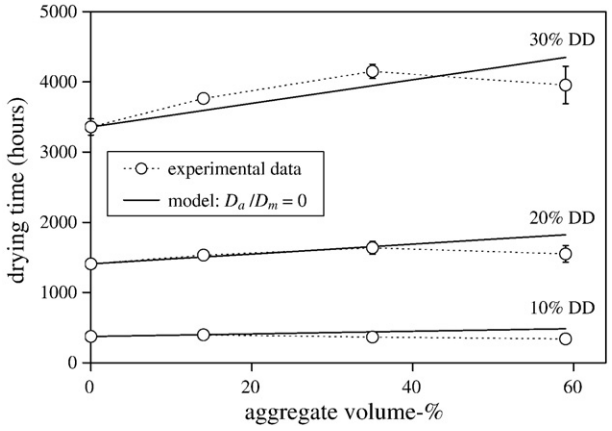

Fig. 7. Effect of aggregate concentration on the drying time (drying rate) of composites with natural sand grains (mono-sized or graded, see Table 1). Number of specimens were as follows for aggregate concentrations of 0% (n=4); 14% (n=1); 35% (n=2); and 59% (n=3) for all stages of drying. Error bars of data points at 10% degree of drying (DD) smaller than the data-icons.

differed in two ways from the glass bead composites (Fig. 7). Firstly, the 'bump' in the experimental curves at low aggregate concentrations was absent. Secondly, the drying times at an aggregate concentration of 59% were much lower in the sand grains composites, and also lower than the predicted values for composites with D_a/D_m=0. Up to an aggregate concentration of 35%, the slopes of the experimental and model curves are similar. The measured higher drying rate at aggregate concentrations of 59% is discussed in Section 4.2.

Composites with 35% EPS beads dried an average factor of 1.5 faster than composites with 35% glass beads (Figs. 6–8). The EPS composites showed larger moisture absorption (~1 g) than the latter composites (Fig. 2), but this difference is too small to explain the differences in drying rates. The higher drying rates appear to be a direct result of the much higher water vapour diffusion coefficient of EPS. The simple model predicts the drying times for Polystyrene bead composites well for a chosen diffusion coefficient ratio D_a/D_m=0.7. The results in Fig. 8 once more clearly illustrate that the first order effect on drying rate is the aggregate diffusivity and concentration, and that the development of drying shrinkage microcracks only had a minor effect. The glass bead composites showed a much higher degree of cracking than the composites with EPS beads, because aggregate-restraint is absent in the latter, while the drying times of the glass bead composites were much higher. Moreover, for the composites with EPS beads the drying rate increased, but the total crack length decreased with increasing aggregate concentration.

4. Discussion

4.1. Effect of microcracks on drying rate

Larger crack length and depth resulted, on average, in slightly higher drying rates to reach 10 and 20% degree of drying (Fig. 4). The crack density measured on a 2D specimen cross-section is however not equal to the true 3D crack density as predicted by quantitative stereology. The difference being a factor π/2; 4/π; or 1, depending on whether microcracks are oriented (i) perpendicular to drying surface; (ii) randomly; or (iii) parallel to the drying surface, respectively [13]. Microcracks due to the development of a steep moisture and shrinkage gradient ('self-restraint'), are mainly perpendicular, and sometimes parallel to the drying surface [13,16]. Aggregate-restraint causes drying shrinkage microcracks with a random orientation [13,14]. In most composites microcracking was a result of a combined effect of self-restraint and aggregate restraint. Relating crack length to real 3D crack density is difficult in those cases since crack surfaces have partly a preferred and partly a random orientation. Moreover, cracks along the interface between matrix and aggregate ('bond cracks') were not measured because their presence is in general hard to judge [13]. The measured total crack length was thus lower than the true crack length including bond cracks and should thus be considered as an approximate measure of the true 3D crack density in the studied composites.

What is the theoretical effect of microcracks on water vapour diffusion in cementitious materials? Bažant and Raftshol [6] calculated that shrinkage (macro)cracks can increase drying diffusivity by several orders of magnitude under the assumptions that cracks are perpendicular to the drying surface and have a constant crack width. In their analyses drying diffusivity was found to be proportional to the crack width cubed and inversely proportional to the crack spacing. In an experimental study the drying diffusivity of concrete was increased a factor 2.25 by cracks with a width of 0.1 mm and a spacing of 70 mm [4]. The theoretically estimated effect of such a crack system on drying diffusivity was however two orders of magnitude larger than the experimental results [4]. They concluded from this that the cracks in the experiments must have been discontinuous in the specimen interior, and are being interconnected by much narrower necks with possible widths in the order of 10 μm that slowed down the moisture transport.

In our experiments, the development of shrinkage microcracks increased the drying rate by a maximum factor of 1.1 relative to the least cracked specimen at 10 and 20% degree of drying (Fig. 4). The slope of the best-fit line through the data points in the crack length and crack depth graphs decreased slightly (i.e., became less negative) from 10 to 20% degree of drying, and was almost horizontal at 30% degree of drying. This means that the effect of microcracks of drying rate was strongest at 10% degree of drying (up to 350–450 h drying) and decreased subsequently, even though the degree of cracking increased with degree of drying. Bažant et al. [4] also measured that cracks only increased drying diffusivity in an initial period of drying (in their large specimens about 130 days). At later stages of drying, the drying rate is mainly limited by the water vapour migration from the uncracked material into the cracks themselves.

It is difficult to make a theoretical estimate of the effect of drying shrinkage microcracking on the drying rate. It is impossible to give average values for the crack width and crack spacing of the crack-patterns in our experiments such as was done in the analyses of Bažant and Raftshol [6]. This is because, due to aggregate-restraint,

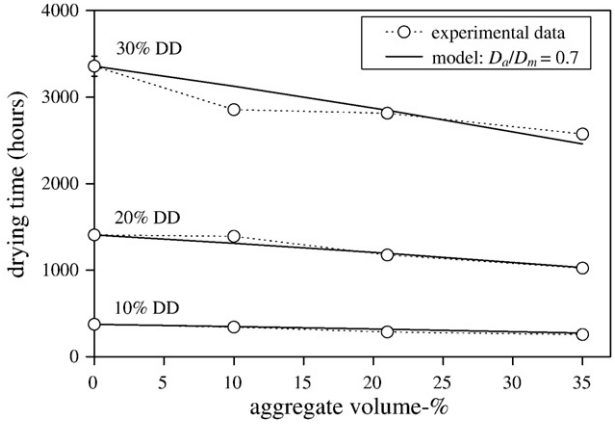

Fig. 8. Effect of aggregate concentration on the drying time (drying rate) of composites with EPS-beads (4 or 6 mm, see Table 1). Number of specimens were as follows for aggregate concentrations of 0% (n=4); 10% (n=1); 21% (n=1); and 35% (n=2) for all stages of drying. Error bars of data points at 35% aggregates smaller than the data-icons. DD is degree of drying.

drying shrinkage microcracks were generally not perpendicular to the drying surface. Moreover, the crack-patterns evolved in time. Suwito et al. [5] give a theoretical estimate of the effect of drying induced damage on moisture (drying) transport properties using a coupled numerical model.

The specimens that showed the highest degree of cracking at 10 and 20% degree of drying, and correspondingly the largest effect on the drying rate, were mixtures with a high degree of shrinkage microcracking due to aggregate restraint. Those mixtures (the G4- and G6-composites) did not contain a graded aggregate content and had much lower aggregate concentrations compared to practical mortars or concretes (Fig. 3). The degree and evolution of drying shrinkage microcracking in the more practical mortar with 59% of Fuller graded sand grains (Nfg-59) was much less [13], and had a negligible effect on the drying rate. From these observations it seems reasonable to conclude that microcracks in practical concretes due internal restraints (i.e., non-uniform drying and aggregate restraint) do not have a significantly feedback affect on the drying rate. Only when drying concrete is externally (substrate) restrained, development of macrocracks may occur that could have a more significant effect on drying rate.

The effect of cracks on the ingress (capillary suction or permeation) of moisture into cementitious materials is probably much larger than the effect on drying diffusivity. This is theoretically predicted [6] and has also been shown experimentally [17]. It can be expected that drying shrinkage microcracks significantly affect the moisture permeation into cementitious materials, even when microcracks (partly) close due to swelling of the material. This is substantiated by the observation that the fluid epoxy (with a higher viscosity than water) easily penetrated microcracks in this study, even in tests without the application of a low under-pressure, i.e., vacuum-impregnation [13].

4.2. Effects of aggregates on drying rate

Aggregate concentration and aggregate diffusivity had significant effects on the drying rate of cementitious composites: Higher concentrations of glass beads or sand grains generally meant lower drying rates, but higher concentrations of EPS-beads lead to higher drying rates. The simple linear diffusion model given in the Appendix predicts that the drying time required to reach a specific degree of drying, is proportional to the total moisture loss divided by the bulk diffusion coefficient ($t \sim m_t/D_{\text{bulk}}$). It predicts the drying times measured in our experiments well. However, cementitious composites with glass beads or sand grains, with equal predictions curves for $Da/Dm=0$, showed some clear differences in drying behaviour. Firstly, glass bead composites showed relatively low drying rates at aggregate volume percentages of 10–14% (Fig. 6), while composites with sand grains showed relatively high drying rates at aggregate volume percentages of 59% (Fig. 7). These differences, especially the first one, are not well understood, but they are believed to be significant because they appear to occur at all three stages of drying. They cannot be explained by differences in moisture absorption during wet-curing of composites prepared with either cement from bag 1 or bag 2. When the drying times are plotted separately for composites prepared from the two cement bags, the two curves do almost overlap. The composites with 59% graded glass beads and sand grains were both prepared from cement bag 2 and showed almost equal moisture absorption (Fig. 2), while the difference in their average drying times to reach 30% degree of drying was 627 h.

The interfacial transition zone (ITZ) surrounding the aggregates could possibly have played a role in the drying process. The amount of ITZ-paste in cementitious composites varies with aggregate size, concentration and grading, but the total amount of this more porous paste should not affect transport properties. This is because an increase in the amount of ITZ-paste means a corresponding decrease of the w/c-ratio (porosity) of the matrix away from the aggregates [3]. We observed that composites with different glass bead sizes, and corresponding differences in the total quantity of ITZ-paste, showed almost no differences in drying rate (Fig. 5). However, when the transition zones of neighboring aggregate particles overlap at high aggregate concentrations and form a percolating network, there might be an effect of the ITZ on transport properties [3,11,12]. In the G- and N-composites with 59% graded aggregates, the aggregate concentration may have been high enough for this so-called ITZ-percolation. Due to the angular shape of sand grains, the probability for overlap and percolation of ITZ in N-composites may have been larger than in G-composites, and this could possibly explain the lower drying times (higher drying rate) of the former.

The simple model predicts the drying time for composites with EPS beads well for a chosen diffusion coefficient ratio $D_a/D_m=0.7$. The water vapour permeability of expanded polystyrene (EPS) is $2.28 \cdot 10^{-12}$ kg/m·s·Pa in the RH range of 0–60% at 20 °C as measured in a standard cup test [18]. The average water vapour permeability of a concrete (with a density of 2137 kg/m^3) measured under the same experimental conditions as the EPS was $6.35 \cdot 10^{-12}$ kg/m·s·Pa [19]. These measurements would give a corresponding water vapour permeability ratio $\mu_{EPS}/\mu_c=0.4$. This value is of the same order of magnitude as $D_a/D_m=0.7$ used in this study to make the model fit the experimental data. Even though, the bulk diffusion coefficients (D_{bulk}) of composites with EPS-beads were smaller, they lost 10, 20, and 30% of their initial moisture contents faster than plain cement paste with the same w/c-ratio, because less water needed to be transported out of the composites with EPS-beads.

5. Conclusions

- Aggregate concentration has two principal effects on the drying rate of cementitious composites. Firstly, a higher aggregate concentration will result in a lower bulk water vapour diffusion coefficient when $D_a/D_m<1$. Secondly, a higher aggregate concentration means that less water needs to diffuse out of the specimen to reach a specific degree of drying. As a result, in cementitious composites with glass beads (with $D_a/D_m=0$), the drying rate continuously decreased with aggregate concentration, while in composites with EPS-beads (with $D_a/D_m \sim 0.7$) the drying rate increased with aggregate concentration. In composites with natural sand, the drying time vs. aggregate concentration curve had a convex shape. Composites with 59% glass beads dried a factor 1.3 slower, while composites with 35% EPS-beads dried a factor 1.4 faster than plain cement paste with the same w/c-ratio.
- Drying shrinkage microcracking had a very small effect on the drying rate of the studied composites, and only in an initial period of drying. The drying rate increased by a maximum factor of about 1.1 for cementitious composites with an extreme degree of drying shrinkage microcracking. In practical mortars and concretes, the composition is such that drying will not lead to high degrees of microcracking due to self-restraint or aggregate restraint. It is therefore to be expected that the development of drying shrinkage microcracks will not have a significant feedback affect on the drying rate of mortars and concretes.

Appendix A

Predicting the drying rate of cementitious composites would require a model based on Fick's second law of diffusion and with D_m being a function of moisture content. Here we give a much more simple linear diffusion model that predicts the drying rates of most of the studied cementitious composites well. We make the very crude assumption that the evolution of the moisture distribution (i.e., the evolution of internal relative humidity) during drying was the same in all composites with equal water-cement ratio. Under this assumption, the diffusion coefficient of the matrix (D_m) averaged over time and

space is equal for all composites. Fick's first law now approximates the drying process:

$$J = -D_{\text{bulk}} \frac{\partial c}{\partial x}$$

where, J is the flux [kg/m^2·s], D_{bulk} is the bulk diffusion coefficient of the composite [m^2/s], c is the water vapour concentration [kg/m^3], x is the specimen thickness [m]. As described above we say that $\partial c/\partial x$ has the same average value (k) for all composites, thus it follows:

$$J = -D_{\text{bulk}} \cdot k$$

In the case of the plain cement specimens $D_{\text{bulk}} = D_m$. At a degree of drying of 10%, the cement paste specimens lost an average 15.1 g water in an average 374 h. Thus:

$$15.1\,\text{g}/0.0064\,\text{m}^2 \cdot 374\,\text{h} = -D_m \cdot k \;\rightarrow\; D_m = -6.31/k$$

We can now calculate the drying time of a glass bead composite ($D_a/D_m = 0$) with an aggregate concentration of 59% required to reach a 10% degree of drying using one of the equation in Fig. 1. If we use Eq. 1 in Fig. 1 we find for the glass bead composite:

$$D_{\text{bulk}} = 0.32 D_m \text{ and,}$$

$$(1 - 0.59) \cdot 15.1\text{g}/0.0064\,\text{m}^2 \cdot t = -D_{\text{bulk}} \cdot k \;\rightarrow\; t = 484\ \text{h}.$$

Thus, the drying time required to reach a specific degree of drying, is here predicted to be proportional to the total moisture loss divided by the bulk diffusion coefficient ($t \sim m_t/D_{\text{bulk}}$). This simple model predicts that composites with 59% glass beads dry a factor 1.3 slower than plain cement paste with the same w/c-ratio. This corresponds well to the average experimental factor of 1.25 for composites with 59% aggregates. The predicted drying times of all composites, relative to the drying time of plain cement paste, required to reach 10, 20 or 30% degree of drying are plotted in Figs. 6–8. For the glass bead and sand grain composites we used ($D_a/D_m = 0$) and got the best fit using Eq. (1) in Fig. 1. Eq. (2) will give drying rates independent of aggregate concentration (i.e., a horizontal line). The use of Eq. (3) will give drying times that are significantly higher than the experimental values for aggregate concentrations above 30% (the same deviation was also found by Shane et al. [3] for mortar conductivities). For the composites with EPS-beads $D_a/D_m = 0.7$ was used, and Eqs. (1) and (2) give similar results. EPS-composites with 35% aggregates dried a factor 1.4 faster than plain cement paste with the same w/c-ratio.

References

[1] Z. Hashin, S. Shtrikman, A variational approach to the theory of the effective magnetic permeability of multiphase materials, Journal of Applied Physics 33 (10) (1962) 3125–3131.
[2] R.M. Christensen, Mechanics of composite materials, Wiley-Interscience, New York, 1979.
[3] J.D. Shane, T.O. Mason, H.M. Jennings, E.J. Garboczi, D.P. Bentz, Effect of the interfacial transition zone on the conductivity of Portland cement mortars, Journal of the American Ceramic Society 83 (5) (2000) 1137–1144.
[4] Z.P. Bažant, S. Sener, J.K. Kim, Effect of cracking on drying permeability and diffusivity of concrete, ACI Materials Journal 84 (1987) 351–358.
[5] A. Suwito, A. Ababneh, Y. Xi, K. Willam, The coupling effect of drying shrinkage and moisture diffusion in concrete, Computers and Concrete 3 (2/3) (2006) 103–122.
[6] Z.P. Bažant, W.J. Raftshol, Effect of cracking in drying and shrinkage specimens, Cement and Concrete Research 12 (1982) 209–226.
[7] S. Jox, C. Becker, G. Meschke, Hygro-mechanical modelling of cracked concrete in the framework of the X-FEM, Proceedings of the 6th Int. Conf. on Fracture Mechanics of concrete and concrete structures (FraMCoS-6), Catania, Italy, 2007, pp. 517–524.
[8] J.F. Daïan, J. Saliba, Transient moisture transport in a cracked porous medium, Transport in Porous Media 13 (1993) 239–260.
[9] M. Mainguy, F.J. Ulm, Coupled diffusion–dissolution around a fracture channel: The solute congestion phenomenon, Transport in Porous Media 80 (2001) 481–497.
[10] K.L. Scrivener, A.K. Crumbie, P. Laugesen, The Interfacial Transition Zone (ITZ) between cement paste and aggregate in concrete, Interface Science 12 (2004) 411–421.
[11] D.N. Winslow, M.D. Cohen, D.P. Bentz, K.A. Snyder, E.J. Garboczi, Percolation and pore structure in mortars and concrete, Cement and Concrete Research 24 (1994) 25–37.
[12] E.J. Garboczi, L.M. Schwartz, D.P. Bentz, Modelling the influence of the interfacial zone on the DC electrical conductivity of mortar, Advanced Cement Based Materials 2 (1995) 169–181.
[13] J. Bisschop, Drying shrinkage microcracking in cement-based materials. Ph.D-thesis Delft University of Technology, Delft University Press, the Netherlands (2002) (ISBN 90-407-2341-9). 208p.
[14] J. Bisschop, J.G.M. Van Mier, Effect of aggregates on drying shrinkage microcracking in cement-based materials, Materials and Structures 35 (2002) 453–461.
[15] J. Bisschop, J.G.M. Van Mier, How to study drying shrinkage microcracking in cement-based materials using optical and scanning electron microscopy? Cement and Concrete Research 32 (2002) 279–287.
[16] J.E. Bolander, S. Berton, Simulation of shrinkage induced cracking in cement composite overlays, Cement & Concrete Composites 26 (2004) 861–871.
[17] C.M. Aldea, S.P. Shah, A. Karr, Effect of cracking on water and chloride permeability of concrete, Journal of Materials in Civil Engineering 11 (3) (1999) 181–187.
[18] G.H. Galbraith, R.C. McLean, J. Guo, Moisture permeability data presented as a mathematical function applicable to heat and moisture transport models, Building Simulation 1997, Prague, Czech Republic, September 8-10 1997, (P200).
[19] G.H. Galbraith, R.C. McLean, J. Guo, Moisture permeability data presented as a mathematical function, Building Research & Information 26 (3) (1998) 157–168.